The double inverted pendulum with real mass distribution stabilization*

Milan Anderle and Sergej Čelikovský [1]

Abstract— **The stabilization of the real laboratory model of the underacuated double inverted pendulum having the actuator placed between its links and a realizable mass distribution adjustment is presented here. More specifically, this laboratory model is to be stabilized at its upper equilibrium with both links being stretched along a single line and pendulum achieving the maximal possible length. This paper presents various methods to design the stabilizing feedback for the double inverted pendulum actuated between its links and then performs optimization of the model with respect to masses distributions to minimize the controller torques. First, the open-loop control taking the double pendulum to the upper equilibrium is computed from various positions using the optimization tool FMINCON to minimize the torque energy with respect to the mass distribution parameters. Then the optimized parameters are used to test both the LQ feedback for local approximate linearization and the partial exact feedback linearization based nonlinear controller. Both simulations and laboratory experiments using a single leg of the walking-like four link experimental model are presented. The optimized mass distribution will be used in the future four-link development to facilitate its walking design.**

I. INTRODUCTION

The main contribution of this paper consists in the real-time implementation study for the various stabilization methods of the double inverted pendulum with a single actuator placed between its links. More specifically, the respective laboratory model is to be stabilized at its upper equilibrium with both links being stretched along a single line and pendulum achieving the maximal possible length. Furthermore, the laboratory model provides realizable mass distribution adjustment used for the actuator torque minimization. The torque efforts will be optimized first with respect to open-loop control to determine the optimal mass distribution. Then various feedback design methods will be applied to the optimized mass distribution model.

The underactuated double inverted pendulum is one of the simplest underactuated mechanical systems consisting of two rigid links and one actuator, which is either placed between the links, or at the contact point with supporting surface. While both actuator placements allow double pendulum stabilization in upper position both with overlapping and upright links, the placement between links allow a simple movement resembling a human walk as well. In the latter case, alternative names, like Acrobot, Compass gait walker or biped, are often used. To control the Acrobot walking, the partial exact feedback linearization method was developed along with rather special and complex procedures of the residual nonlinearity adjustement [1], [2], [3], [4], [5]. The reason for that complexity was that the nonlinearity influence can not be neglected when nontrivial walking-like trajectory is to be tracked. Yet, for a local stabilization at an equilibrium, a linear feedback based on approximate linearization model might be sufficient while global stabilization still may need a more sophisticated treatment.

Even though the double pendulum with a single actuator placed between the links is the classical mechanical system with many applications, it can also serve as a simple test bed for verifications of feedback control algorithms for underactuated walking robots. Consider a different posture of the inverted pendulum, specifically, the free unconnected ends of each link touch the ground and the mutually connected ends equipped with an actuator are above the ground. Indeed the Acrobot is perhaps the simplest underactuated mechanical system capable to move (at least theoretically) in a way resembling a human walk. However, from practical point of view, an additional movable joint serving as a knee equipped with an actuator has to be added into each link in order to bend the link during the step. This mechanical system is in the literature usually called as the **four-link**, some approaches on its walking-like movement were presented in [6], [7], [8]. The experimental model of the underactuated walking-like mechanical system was built in our laboratory, first as the four-link, later with added torso to have five degrees of freedom, see [3], [4], [5] for description and simple experiments.

In spite of the fact that the Spong's papers on the Acrobot feedback linearization [9], [10], [11] were published almost thirty years ago, the Acrobot control still belongs in active resarch field. In [12] the swing-up and stabilization problem for the Acrobot is solved via the stable manifold method for optimal control, which numerically solves Hamilton-Jacobi equations. The posture control problem of a two-link free flying Acrobot with nonzero initial angular momentum is studied in [13]. An optimal control system design for the Acrobot using inverse linear quadratic design method is proposed in [14].

Due to the nonlinearities of the respective Acrobot model, partial exact feedback linearization, fuzzy based control [15], [16] or sliding mode based control [17], [18] methods (to name a few) were used to analyze them and to design the respective controllers at its whole range of movement except stabilization. The partial exact feedback linearization of the Acrobot was presented first in [9], [10], where two application examples of partial feedback linearization applied to the Acrobot were presented. The first one, called

*The work of Milan Anderle and Sergej Čelikovský was supported by the Czech Science Foundation through the research grant No. 21-03689S.

[1]Milan Anderle and Sergej Čelikovský are with The Czech Academy of Sciences, Institute of Information Theory and Automation
anderle@utia.cas.cz, celikovs@utia.cas.cz

as the collocated linearization, is based on the linearizing output being the actuated angle, whereas the second one, called as the non-collocated linearization, corresponds to the linearizing output being the unactuated angle. Yet, both linearizations have only 2-dimensional linear part and 2-dimensionalresidual nonlinear dynamics. In [19] a special normal form of the Acrobot with linear part having dimension 3 and 1-dimensional residual nonlinear dynamics was presented. Based on that, [1], [2] the respective partial exact feedback linearization of order 3 of the Acrobot was presented and used in [2] to stabilize exponentially the Acrobot, moreover, a large region of attraction was obtained . In [20], [21], [6] the approach from [2] was further extended.

As already mentioned briefly before, the aim of the current paper is to study possibly optimal mass distribution of the legs of walking-like four-link laboratory model which will be used in the future four-link development to facilitate its walking design. To do so, the torque efforts will be optimized first with respect to open-loop control to determine the optimal mass distribution, optimization will use the FMINCON package. This optimization requires yet another approximate linearization of the residual nonlinear dynamics of the respective partial exact feedback linearization, tentatively called the **linearization in linearized coordinates**. Various feedback design methods will be then applied to the respective optimized mass distribution model. Indeed, this paper either newly presents, or repeats various methods to design the stabilizing feedback for the double inverted pendulum actuated between its link, aka Acrobot. More specifically, by virtue of the partial exact feedback linearization and corresponding linearized coordinates and virtual inputs, yet another control method to stabilize the double inverted pendulum in its upper position is proposed in the current paper. For comparision, the LQ controller fo the Acrobot approximate linearization will be applied as well. All studies are performed both in simulations and using a single leg of the walking like four-link built in our laboratory.

The rest of the paper is organized as follows. The next section contains some preliminaries, namely, the derivation of the Acrobot model, its partial exact feedback linearization and approximate linearized model around the upper equilibrium, description of the laboratory model is also included here. Section III numerically optimizes the Acrobot mechanical parameters to minimize the actuator torque during its open loop steering to the upper equilibrium. Section IV presents feedback stabilization and tests it both in simulations and laboratory experiment for the previously obtained optimal values of mechanical parameters, various feedback designs are compared here. Conclusions are drawn in the final section.

II. PRELIMINARIES

A. Dynamical model of the Acrobot

The well-known Euler-Lagrange approach, see [22], [23] will be used here. First, for the mechanical system to be modelled, define generalized coordinates q and generalized velocities $\dot{q}$ and their function - Lagrangian $\mathscr{L}(q,\dot{q})$ given

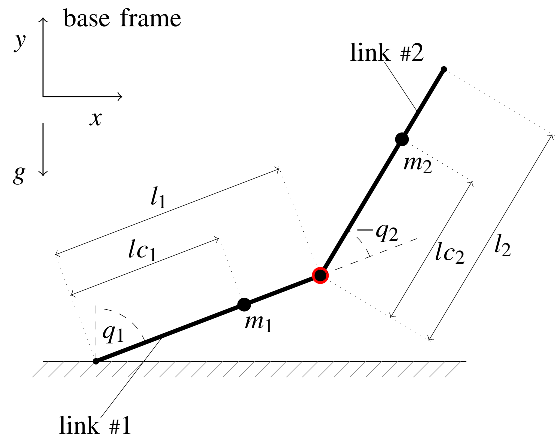

Fig. 1. Geometry of Acrobot

by the difference between the system kinetic energy $\mathscr{K}(q,\dot{q})$ and its potential $\mathscr{P}(q)$ energy, namely

$$\mathscr{L}(q,\dot{q}) = \mathscr{K}(q,\dot{q}) - \mathscr{P}(q). \tag{1}$$

The kinetic energy is typicaly given using the so-called **inertia (aka mass) matrix** as

$$\mathscr{K}(q,\dot{q}) = \dot{q}^\top D(q)\dot{q}, \quad D(q)^\top = D(q) > 0.$$

Euler-Lagrange formalism then provides ordinary differential equations (ODE) describing the time evolution of the modelled mechanical system as follows

$$\frac{d}{dt}\frac{\partial \mathscr{L}}{\partial \dot{q}} - \frac{\partial \mathscr{L}}{\partial q} = \tau$$

where τ are respective external forces acting along generalized coordinates q.

For the Acrobot, schematically depicted in Fig. 1, Euler-Lagrange formalism is applied as follows. Let the generalized coordinates be the angles q_1, q_2 shown in Fig. 1 and τ_2 actuates directly the angle q_2, while the angle q_1 is unactuated. Then, after straightforward, though laborious computation of the respective kinetic and potential energies (detailed are ommited, cf. [22]), the following second-order ODE is obtained

$$\begin{bmatrix} \frac{d}{dt}\frac{\partial \mathscr{L}}{\partial \dot{q}_1} - \frac{\partial \mathscr{L}}{\partial q_1} \\ \frac{d}{dt}\frac{\partial \mathscr{L}}{\partial \dot{q}_2} - \frac{\partial \mathscr{L}}{\partial q_2} \end{bmatrix} = u = \begin{bmatrix} 0 \\ \tau_2 \end{bmatrix}, \tag{2}$$

where u stands for the vector of the external controlled forces. System (2) is the so-called underactuated mechanical system having the degree of the underactuation equal to one. Equation (2) leads to the second-order ODE in the form

$$D(q)\ddot{q} + C(q,\dot{q})\dot{q} + G(q) = u = [0, \tau_2]^\top, \tag{3}$$

where $D(q)$ is the mentioned before inertia matrix, $D(q) = D(q)^\mathrm{T} > 0$, matrix $C(q,\dot{q})$ contains Coriolis and centrifugal terms, vector $G(q) = \frac{\partial \mathscr{P}}{\partial q}$ contains gravity terms. For the simplicity, friction is not considered here.

In the real laboratory model, the links have mass distributed over the length of the link with some extra added concentrated masses. This setting can be equivalently represented as in Figure 1 where links are mass-less, their overall masses are placed at their centres of mass (COM) and they have some moments of inertia with respect to those COM. Introduce the following parameters

$$\begin{aligned}\theta_1 &= m_1 l_{c1}^2 + m_2 l_1^2 + I_{1zz}, \quad \theta_2 = m_2 l_{c2}^2 + I_{2zz}, \\ \theta_3 &= m_2 l_1 l_{c2}, \quad \theta_4 = m_1 l_{c1} + m_2 l_1, \quad \theta_5 = m_2 l_{c2},\end{aligned} \tag{4}$$

where m_1, m_2 is the mass of the link #1, #2, respectively, l_1, l_2 is length of the link #1, #2, respectively, l_{c1}, l_{c2} is the distance to the center of mass of the link #1, #2, respectively, I_{1zz}, I_{2zz} is the moment of inertia about center of mass of the link #1, #2, respectively, g is gravity acceleration, q_1 is the angle that link #1 makes with the vertical, q_2 is the angle that link #2 makes with the link #1, τ_2 is torque applied at the joint between links #1 and #2. The matrices $D(q)$, $C(q,\dot{q})$ and vector $G(q)$ from dynamical equation (3) with material parameters $\theta_{1,2,3,4,5}$ (4) are then determined as follows

$$D(q) = \begin{bmatrix} \theta_1 + \theta_2 + 2\theta_3 \cos q_2 & \theta_2 + \theta_3 \cos q_2 \\ \theta_2 + \theta_3 \cos q_2 & \theta_2 \end{bmatrix}, \tag{5}$$

$$C(q,\dot{q}) = \begin{bmatrix} -\theta_3 \sin q_2 \dot{q}_2 & -(\dot{q}_1 + \dot{q}_2)\theta_3 \sin q_2 \\ \theta_3 \sin q_2 \dot{q}_1 & 0 \end{bmatrix}, \tag{6}$$

$$G(q) = \begin{bmatrix} -\theta_4 g \sin q_1 - \theta_5 g \sin(q_1 + q_2) \\ -\theta_5 g \sin(q_1 + q_2) \end{bmatrix}. \tag{7}$$

Summarizing, throughout the rest of the paper, the model (3), (5), (6), (7) will be analyzed and used.

B. Approximate linearization of the Acrobot

For the second-order ODE (3) denote

$$\tilde{D}(\pi/2, 0) = \begin{bmatrix} \theta_1 + \theta_2 + 2\theta_3 & \theta_2 + \theta_3 \\ \theta_2 + \theta_3 & \theta_2 \end{bmatrix}, \tag{8}$$

$$\tilde{C}(\pi/2, 0, 0, 0) = \begin{bmatrix} 0 & 0 \\ 0 & 0 \end{bmatrix}, \tag{9}$$

$$\tilde{G}(\pi/2, 0) = \begin{bmatrix} -\theta_4 g - \theta_5 g \\ -\theta_5 g \end{bmatrix}. \tag{10}$$

Straightforward computations show that the standard Acrobot model representation as the four-dimensional first-order ODE has locally around its upper equilibrium $q_1 = \pi/2$, $q_2 = 0$, $\dot{q}_1 = \dot{q}_2 = 0$ the following approximate linearization (AL)

$$\dot{x} = Ax + B\bar{u}, \quad x = [x_1, x_2, x_3, x_4]^\top := [q_1, q_2, \dot{q}_1, \dot{q}_2]^\top,$$

$$\bar{u} = [0, 0, 0, \tau_2]^\top,$$

$$A = \begin{bmatrix} \begin{bmatrix} 0 & 0 \\ 0 & 0 \end{bmatrix} & \begin{bmatrix} 1 & 0 \\ 0 & 1 \end{bmatrix} \\ \tilde{D}^{-1}\tilde{G} & \begin{bmatrix} 0 & 0 \\ 0 & 0 \end{bmatrix} \end{bmatrix}, \; B = \begin{bmatrix} \begin{bmatrix} 0 \\ 0 \end{bmatrix} \\ \tilde{D}^{-1} \begin{bmatrix} 0 \\ 1 \end{bmatrix} \end{bmatrix}, \tag{11}$$

and LQR $\tau_2 = K_1 q_1 + K_2 \dot{q}_1 + K_3 q_2 + K_4 \dot{q}_2$, where K_1, K_2, K_3, K_4 are easily computable gains, stabilizes the Acrobot locally exponentially around its upper equilibrium.

C. Partial exact feedback linearization of the Acrobot

Unlike the above derived AL, the **exact feedback linearization (EFL)**, if available, attenuates the nonlinearities exactly, providing thereby better performance of the subsequent controller design. For the Acrobot, only the so-called **partial** EFL is available. More specifically, the largest EFL linearizable part is three dimensional, while the residual nonlinear part is almost linear and simple, for details see [2]. This property goes back to normal forms obtained in [19].

The well-known and convenient concept to obtain partial EFL is the auxiliary output function called as the linearizing output. The Acrobot model provides two independent functions enabling to define variety of the relative degree 3 linearizing outputs, namely the functions denoted σ, p:

$$\sigma = \frac{\partial \mathscr{L}}{\partial \dot{q}_1} = (\theta_1 + \theta_2 + 2\theta_3 \cos q_2)\dot{q}_1 + (\theta_2 + \theta_3 \cos q_2)\dot{q}_2, \tag{12}$$

$$p = q_1 + \frac{q_2}{2} + \frac{2\theta_2 - \theta_1 - \theta_2}{\sqrt{(\theta_1 + \theta_2)^2 - 4\theta_3^2}} \arctan \left(\sqrt{\frac{\theta_1 + \theta_2 - 2\theta_3}{\theta_1 + \theta_2 + 2\theta_3}} \tan \frac{q_2}{2} \right). \tag{13}$$

Indeed, straightforward computations show that for any real constants c_1, c_2, the output defined as $c_1\sigma + c_2 p$ has well-defined relative degree equal to three. Moreover, by (12,13) and some straightforward, though laborious computations, the following relation holds

$$\dot{p} = d_{11}(q_2)^{-1}\sigma, \tag{14}$$

where $d_{11}(q_2) = (\theta_1 + \theta_2 + 2\theta_3 \cos q_2)$ is the corresponding element of the inertia matrix D in (3).

Using the above favorable properties it was shown in [2] that defining the following state space transformation

$$\xi = \mathscr{T}(q, \dot{q}): \quad \xi_1 = p, \quad \xi_2 = \sigma, \quad \xi_3 = \dot{\sigma}, \quad \xi_4 = \ddot{\sigma} \tag{15}$$

and applying (15), (14)to (3), the Acrobot model is transformed into the following dynamics partial EFL form

$$\begin{aligned}\dot{\xi}_1 &= d_{11}(q_2)^{-1}\xi_2, \quad \dot{\xi}_2 = \xi_3, \quad \dot{\xi}_3 = \xi_4, \\ \dot{\xi}_4 &= \alpha(q,\dot{q})\tau_2 + \beta(q,\dot{q}) = w\end{aligned} \tag{16}$$

with the new coordinates ξ and the input w being well defined wherever $\alpha(q,\dot{q})^{-1} \neq 0$. The new input w is a virtual input in ξ coordinates. As a result of this, it is necessary to recompute the virtual input w in ξ coordinates to the real input u in $q, \dot{q}$ coordinates before applying the virtual input on the real model of the Acrobot.

Assume that an open loop control $w^r(t)$, generates a suitable reference trajectory in partial exact linearized coordinates (16). In other words, our task is to track the following reference system

$$\dot{\xi}_1^r = d_{11}^{-1}(q_2^r)\xi_2^r, \quad \dot{\xi}_2^r = \xi_3^r, \quad \dot{\xi}_3^r = \xi_4^r, \quad \dot{\xi}_4^r = w^r. \tag{17}$$

Denoting $e := \xi - \xi^r$ and subtracting (17) from (16) one obtains

$$\begin{aligned} \dot{e}_1 &= d_{11}^{-1}(\phi_2(\xi_1,\xi_3))\xi_2 - d_{11}^{-1}(\phi_2(\xi_1^r,\xi_3^r))\xi_2^r, \\ \dot{e}_2 &= e_3, \quad \dot{e}_3 = e_4, \quad \dot{e}_4 = w - w^r. \end{aligned} \tag{18}$$

Straightforward computations based on the Taylor expansions give

$$\begin{aligned} \dot{e}_1 &= \mu_2(t)e_2 + \mu_1(t)e_1 + \mu_3(t)e_3 + o(e), \\ \dot{e}_2 &= e_3, \quad \dot{e}_3 = e_4, \quad \dot{e}_4 = w - w^r, \end{aligned} \tag{19}$$

where $\mu_1(t), \mu_2(t), \mu_3(t)$ are known smooth time functions bounded from bellow and above, see [2]. Using these properties [20], [2] provide feedback to stabilize the above error dynamics.

D. Description of the real laboratory model

A simple model of the underactuated walking-like mechanical system was built and developed in our laboratory, see Fig. 2 for a brief idea. [3] provides a detailed description with simple leg movement experiment. Sensors of angular positions, velocities and input current measurements for DC motors are used. In contrast to simulation only, the real measured signals are corrupted with noise and therefore its filtering is, indeed, necessary. To do so, in [4] the Extended Kalman Filter was proposed and off-line verified using data obtained during a simple movement of one leg. In [5] the EKF was implemented using operations available on a low cost hardware and successfully verified in an application of on-line data processing.

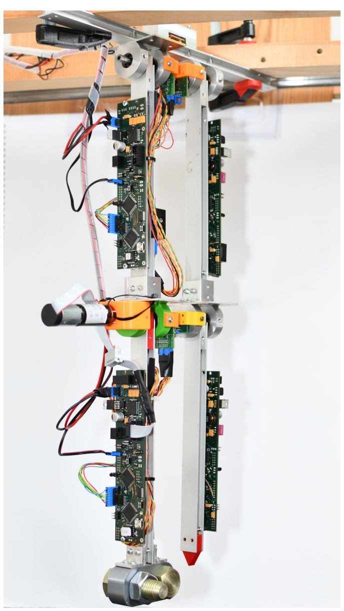

Fig. 2. Real four link walking robot. The left leg is equipped with an additional weight such that the controllability condition is fulfilled. The second leg is not in use here, therefore it is disconnected.

Physical quantities that describe the model of the robot leg together with its values are summed up in Table I. The values were either measured, especially length or mass of a link, or calculated especially center of mass or inertia of each link. In Figure 3 one can see a comparison of real links movement (dotted black line) from an initial point without any control input with a simulation of two link movement (blue solid line) with parameters given in Table I from the same initial point. As one can see the identified mechanical parameters fit the real model very well. The inertial of bottom link takes into the account the mass of bottom link with the added mass and their displacement.

TABLE I

IDENTIFIED PARAMETERS OF THE DOUBLE PENDULUM MODEL

l_1, l_2	length of each link	0.27	$[m]$
l_{c1}	center of gravity of upper link	0.23	$[m]$
l_{c2}	center of gravity of bottom link	0.24	$[m]$
m_1	mass of upper link	0.50	$[kg]$
m_2	mass of bottom link	0.12	$[kg]$
I_1	inertia of upper link	0.00256	$[m^2 Kg]$
I_2	inertia of bottom link	0.00255	$[m^2 Kg]$
m_{added}	added mass at the end of the bottom link	0.54	$[kg]$

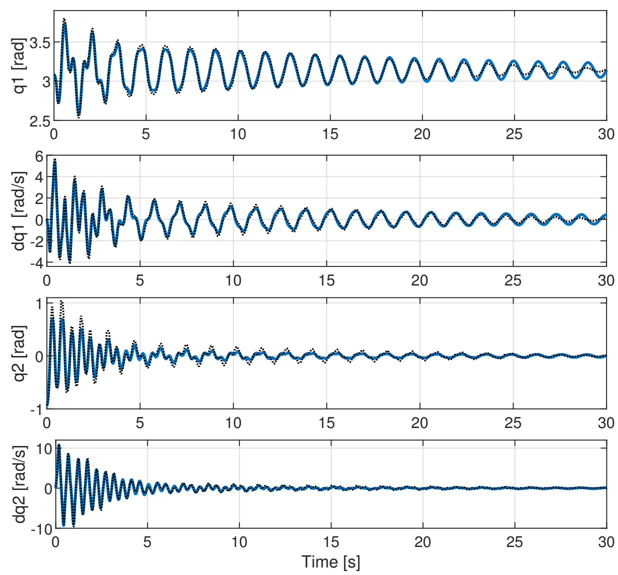

Fig. 3. Comparision of real movement with simulations.

III. PENDULUM MODEL PARAMETERS TUNING

The focus in this section is on pendulum model parameters tuning such that the following controllability condition is fulfilled

$$\theta_5(\theta_1 + \theta_3) \neq \theta_4(\theta_2 + \theta_3), \tag{20}$$

where $\theta_{1,2,3,4,5}$ are given by (4). The controllability conditions is given as the full rank condition of the controllability matrix of the linearized system (11). The mechanical parameters of the real model except the added mass m_{added} given in Table I do not fulfill the controllability condition resulting in simulations of the double inverted pendulum stabilization in the upper equilibrium as depicted in Figure 4. Numerical optimization of the mechanical parameter is performed here in order to (20) is fulfilled and, moreover, the required torque of the attached actuator is minimal such that the actuator is capable to stabilize the real Acrobot model in the upper equilibrium even after small deflection. The real pendulum model and its control is taken into the account, therefore the opportunities to any change of the mechanical parameters are limited to putting an additional mass on the pendulum link in a specific position. The *FMINCON* solver is used to find the optimal value of the additional mass with respect to the controllability condition (20) and minimal torque. Due to a design requirements and limitations, the additional mass is placed at the end of the second link. To do so, yet another coordinates are introduced in the next subsection in order to the *FMINCON* solver can be used. Nevertheless, in the case of the double inverted pendulum with unrealistic mass displacement, i.e. the almost massless links with the mass placed in the ends of each link including mass and length given in Table I, the controllability condition (20) is fulfilled and therefore its stabilization in the upper equilibrium is sufficient, see Figure 5.

In Figures 4,5,7 the blue courses correspond in (a) to angular positions q_1 and in (b) to angular velocities $\dot{q}_1$ whereas the red courses correspond in (a) to angular positions q_2 and in (b) to angular velocities $\dot{q}_2$.

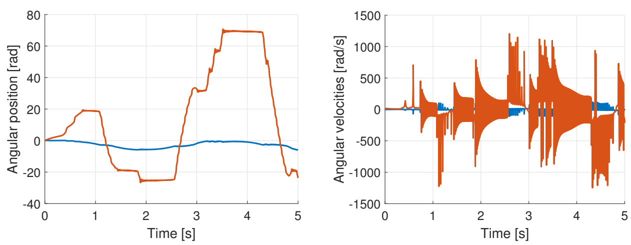

(a) (b)

Fig. 4. Stabilization response for (a) angular positions $q_{1,2}$, (b) angular velocities $\dot{q}_{1,2}$ for double inverted pendulum with real mass distribution according to the real laboratory model.

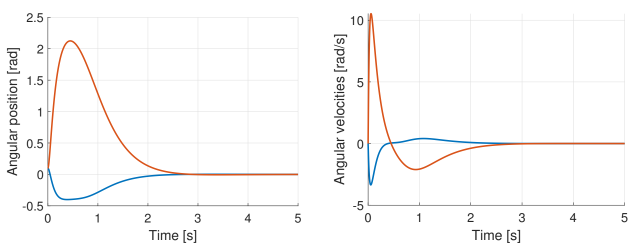

(a) (b)

Fig. 5. Stabilization response for (a) angular positions $q_{1,2}$, (b) angular velocities $\dot{q}_{1,2}$ with unreal mass distribution, i.e. massless links with mass in the end of the link.

A. Linearization in linearized coordinates

In [24] the *FMINCON* solver was used to numerical tuning of mechanical parameters of a five-link walking biped. In [25] the numerical tuning of mechanical parameters of an Acrobot with a torso was performed in ξ coordinates (15) using the *FMINCON* solver by virtue of linear Acrobot dynamics caused by the torso, i.e. $\dot{\xi}_1 = \xi_2,\ \dot{\xi}_2 = \xi_3,\ \dot{\xi}_3 = \xi_4,\ \dot{\xi}_4 = \alpha(q,\dot{q})\tau_2 + \beta(q,\dot{q}) = w$.

The linearized Acrobot dynamics (16) in ξ coordinates (15) also represents the double inverted pendulum dynamics with the actuator between the links and therefore the *FMINCON* solver can be used here as well as in [25]. In contrast to linear dynamics of the Acrobot with torso in [25], the linearized Acrobot dynamics (16) has a nonlinear therm $d_{11}(q_2)$ (5) in the first line to be linearized in the upper equilibrium.

The linearized form in upper equilibrium is straightforward $d_{11}^{lin} = \theta_1 + \theta_2 + 2\theta_3$ and results in following linearized system in the linearized coordinates (16)

$$\tilde{\tilde{A}} = \begin{pmatrix} 0 & 1/d_{11}^{lin} & 0 & 0 \\ 0 & 0 & 1 & 0 \\ 0 & 0 & 0 & 1 \\ 0 & 0 & 0 & 0 \end{pmatrix}, \quad \tilde{\tilde{B}} = \begin{pmatrix} 0 \\ 0 \\ 0 \\ 1 \end{pmatrix}, \tag{21}$$

$$\tilde{\tilde{C}} = \mathrm{diag}(1,1,1,1), \quad \tilde{\tilde{D}} = [0,0,0,0]' \tag{22}$$

according to the state vector $[\xi_1^{\rm lin}, \xi_2^{\rm lin}, \xi_3^{\rm lin}, \xi_4^{\rm lin}]'$. Resulting in the following linearized Acrobot's dynamics (16) in an neighbourhood of the upper equilibrium corresponding to the double inverted pendulum dynamics

$$\dot{\xi}_1^{\rm lin} = (d_{11}^{\rm lin})^{-1}\xi_2^{\rm lin},\ \dot{\xi}_2^{\rm lin} = \xi_3^{\rm lin},\ \dot{\xi}_3^{\rm lin} = \xi_4^{\rm lin},\ \dot{\xi}_4^{\rm lin} = w^{\rm lin}. \tag{23}$$

B. Mechanical parameters optimization

To find the optimal value of the added mass, denoted here as parameter x, the nonlinear programming solver *FMINCON* was used as follows

x = *fmincon(costFunction,*x_0*,[],[],[],[],*l_b*,*u_b*,nonlConstr)*,

where $costfunction(x)$ is the criterion to optimize: $\sum_{i=0}^{k-1} w_i^2$, w is virtual input in ξ coordinates (16), x_0 is some initial parameter guess, l_b, u_b are lower and upper bounds type constraints $l_b \leq x_0 \leq u_b$ and *nonlConstr* is the nonlinear constraints represents controllability condition (20). The optimization problem also depends on the boundary conditions $\xi(0) = \xi_{in}, \xi(T) = \xi_{fin}$ corresponding to the initial pendulum states $q(0), \dot{q}(0)$ and final pendulum states $q(T), \dot{q}(T)$ at time $t = T$.

In Figure 6 (a) one can see the course of open loop control $w^{\rm lin}$ whereas in (b) one can see courses of corresponding linearized coordinates $\xi_{1,2,3,4}^{\rm lin}$ as an output of the *FMINCON* solver for initial pendulum states $q_1(0) = 0, q_2(0) = 0, \dot{q}_1(0) = 0.05, \dot{q}_2(0) = 0$ and final pendulum states $q_1(T) = 0, q_2(T) = 0, \dot{q}_1(T) = 0.05, \dot{q}_2(T) = 0$ for total time $T = 1$ s. Corresponding courses in $q, \dot{q}$ coordinates are depicted in Figure 7 (a) and (b) also obtained as an open loop control of the double inverted pendulum from the initial state using $w^{\rm lin}$ recomputed into τ_2, i.e. $\tau_2 = (w - \beta(q,\dot{q}))/\alpha(q,\dot{q})$ (16). Moreover, the value of additional mass founded by the *FMINCON* solver as $x = 0.4513$ Kg was considered in the open loop simulations. Several runs of the optimizing solver was consider with different initial pendulum states and different initial value of x_0, nevertheless, the value of additional mass equal to $x = 0.4513$ Kg is a local minimum of the optimization problem.

The linearized coordinates and corresponding dynamics (23) are also applicable to a feedback stabilization of the

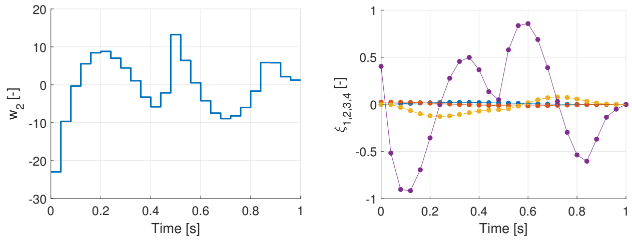

(a) (b)

Fig. 6. Stabilization response for (a) open loop control w^{lin}, (b) linearized coordinates $\xi^{\text{lin}}_{1,2,3,4}$.

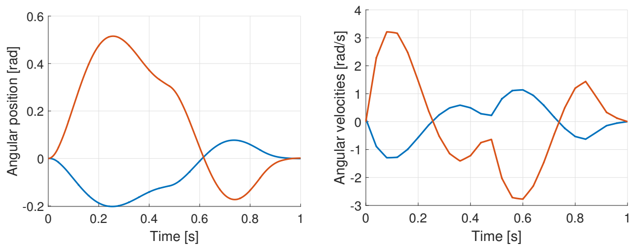

(a) (b)

Fig. 7. Open loop control of double inverted pendulum (a) angular positions $q_{1,2}$, (b) angular velocities $\dot{q}_{1,2}$ with real mass distribution and added mass at the end of the upper link.

double inverted pendulum in the upper equilibrium design. To do so, consider the feedback in ξ^{lin} coordinates as follows $w = K_1\xi^{\text{lin}}_1 + K_2\xi^{\text{lin}}_2 + K_3\xi^{\text{lin}}_3 + K_4\xi^{\text{lin}}_4$ with gains $K_{1,2,3,4}$ given by the Linear-Quadratic Regulator approach. The simulation of stabilization of the double inverted pendulum with real mass distribution according to the real laboratory model and with added mass $m = 0.4513\,\text{Kg}$ to the end of the upper link is depicted in Figures 8 (a), (b). The blue courses correspond in (a) to angular positions q_1 and in (b) to angular velocities $\dot{q}_1$ whereas the red courses correspond in (a) to angular positions q_2 and in (b) to angular velocities $\dot{q}_2$. To be clear, the feedback gains were design using the linearized pendulum's dynamics (23) and applied on the pendulum model via virtual input w recomputed to the real input τ to be applied on the pendulum model in $q, \dot{q}$ coordinates (16).

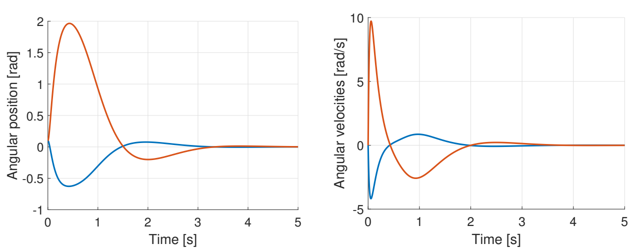

(a) (b)

Fig. 8. Stabilization response for (a) angular positions $q_{1,2}$, (b) angular velocities $\dot{q}_{1,2}$ for double inverted pendulum with real mass distribution according to the real laboratory model and added mass $m = 0.4513\,\text{Kg}$ in the end of the upper link.

IV. SIMULATIONS AND EXPERIMENTS

In this section simulation and experimental results of the double inverted pendulum control in the upward position are presented. The value of the additional mass used in simulations or in experiment is slightly different from the value fouded by the *FMINCON* solver because the additional mass is composed of two high-strength bolts together with a frame as can be seen in Figure 2. Nevertheless, the controllability condition is fulfilled.

A. Simulations

The proposed feedback control methods were applied on the Acrobot model in the upper equilibrium to stabilize it with an initial error in angular position q_2. In the simulations, the mechanical parameters of the Acrobot model from Table I together with the additional mass at the end of the upper link were used. The results are depicted in Figures 9 and 10 for LQR control based on linearized Acrobot model and the partial exact feedback linearization based feedback, respectively. In Figure 11 are depicted corresponding courses of torques.

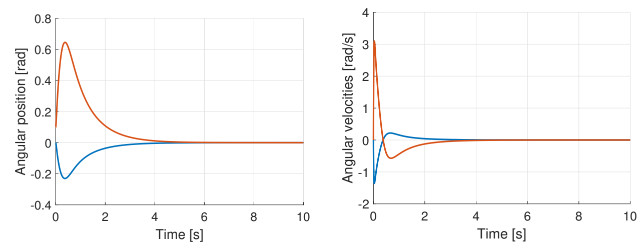

(a) (b)

Fig. 9. Simulations: Stabilization response (a) angular positions $q_{1,2}$, (b) angular velocities $\dot{q}_{1,2}$ for the control approach based on the Acrobot linearization in upper equilibrium and LQ controller based design.

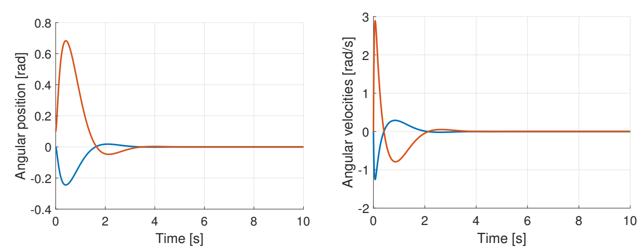

(a) (b)

Fig. 10. Simulations: Stabilization response (a) angular positions $q_{1,2}$, (b) angular velocities $\dot{q}_{1,2}$ for the control approach based on the partial feedback linearization.

B. Experiments

The feedback control method based on the linearized form of the Acrobot in the upper equilibrium with added mass was also verified in the simple real application of stabilization of the Acrobot featuring as the double inverted pendulum in the upper equilibrium. The courses of angular positions q_1 and q_2 are depicted in Figure 12(a), (b).

Certain stabilization in the upper equilibrium without any external disturbances was achieved. Nevertheless, improvement of signals filtering and/or DC motor controller tuning is necessary before performing another experiments.

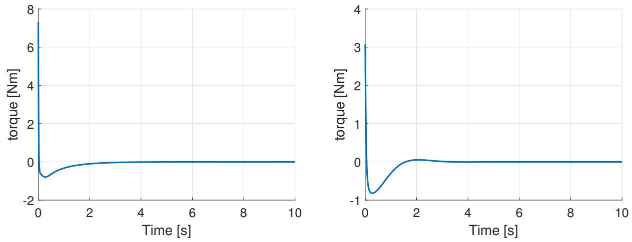

(a) (b)

Fig. 11. Simulations: (a) torque for the control approach based on the Acrobot linearization in upper equilibrium and LQ controller based design, (b) torque for the control approach based on the partial feedback linearization.

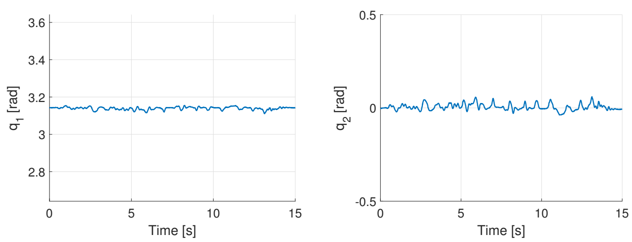

(a) (b)

Fig. 12. Experiment: Stabilization response for angular positions (a) q_1 and (b) q_2.

V. CONCLUSIONS

To analyze future optimal mass distributions of the four-link walking-like system, the stabilization of its single leg, as if being the double inverted pendulum actuated between links (aka Acrobot), at its upper equilibrium with added mass at the end of the upper link was tested both in simulations and in the real-time experiments. The LQ feedback control based on the AL around its upper equilibrium, together with partial EFL based control methods, were completed by the method using further linearization of the residual nonlinear dynamics of the partial EFL.

The last method also provides possiblity to optimize the Acrobot mass distribution using *FMINCON* solver, which is capable to find the optimal additional mass to be placed at the end of the upper link. Respective parameters comply with required constraints and provide minimization of the actuator open-loop control efforts. The optimal parameters are then used in all previously mentioned feedback controllers tests.

REFERENCES

[1] J. Zikmund, S. Čelikovský, and C. Moog, "Nonlinear control design for the Acrobot," in *Preprints of the 3rd IFAC Symposium on Systems Structure Control*, Foz do Iguassu, Brazil, 2007.

[2] S. Čelikovský, J. Zikmund, and C. Moog, "Partial exact linearization design for the Acrobot walking," in *Preprints of the American Control Conference, 2008*, Seattle, USA, 2008, pp. 874–879.

[3] M. Anderle, S. Čelikovský, and K. Dolinský, "Simple model of underactuated walking robot," in *2015 10th Asian Control Conference (ASCC)*, Kota Kinabalu, MY, May 2015, pp. 1–6.

[4] M. Anderle and S. Čelikovský, "On the sensor fusion in the walking robots design," in *2017 11th Asian Control Conference (ASCC)*, Gold Coast, AU, Dec 2017, pp. 2534–2539.

[5] ——, "Sensor fusion for simple walking robot using low-level implementation of Extended Kalman Filter," in *IFAC Conference on Modelling, Identification and Control of Nonlinear Systems - IFAC MICNON 2018*, Guadalajara, Mexico, 2018.

[6] S. Čelikovský, M. Anderle, and C. Moog, "Embedding the Acrobot into a general underactuated n-link with application to novel walking design," in *Proceedings of the Europen Control Conference, ECC 2013*, Zurich, Switzerland, 2013, pp. 682–689.

[7] S. Čelikovský and M. Anderle, "On the collocated virtual holonomic constraints in Lagrangian systems," in *2016 American Control Conference (ACC)*, July 2016, pp. 6030–6035.

[8] ——, "Collocated virtual holonomic constraints in Hamiltonian formalism and their application in the underactuated walking," in *2017 11th Asian Control Conference (ASCC)*, Gold Coast, AU, Dec 2017, pp. 192–197.

[9] M. Spong, "Partial feedback linearization of underactuated mechanical systems," in *Intelligent Robots and Systems '94. 'Advanced Robotic Systems and the Real World', IROS '94. Proceedings of the IEEE/RSJ/GI International Conference on*, vol. 1, 1994, pp. 314–321 vol.1.

[10] ——, "Partial feedback linearization of underactuated mechanical systems," in *Proceedings of the IEEE/RSJ/GI International Conference on Intelligent Robots and Systems '94. 'Advanced Robotic Systems and the Real World'*, vol. 1, 1994, pp. 314–321.

[11] ——, "Underactuated mechanical systems," in *Control Problems in Robotics and Automation*, ser. Lecture Notes in Control and Information Sciences, B. Siciliano and K. Valavanis, Eds. Springer Berlin / Heidelberg, 1998, vol. 230, pp. 135–150, 10.1007/BFb0015081. [Online]. Available: http://dx.doi.org/10.1007/BFb0015081

[12] T. Horibe and N. Sakamoto, "Nonlinear optimal control for swing up and stabilization of the acrobot via stable manifold approach: Theory and experiment," *IEEE Transactions on Control Systems Technology*, vol. 27, no. 6, pp. 2374–2387, 2019.

[13] X. Xin, T. Mita, and M. Kaneda, "The posture control of a two-link free flying acrobot with initial angular momentum," *IEEE Transactions on Automatic Control*, vol. 49, no. 7, pp. 1201–1206, 2004.

[14] N. Hannouda and H. Takami, "Control of acrobot using inverse linear quadratic method," in *2018 International Conference on Control, Automation and Diagnosis (ICCAD)*, 2018, pp. 1–4.

[15] Z. Ben Hazem, M. J. Fotuhi, and Z. Bingul, "Anti-swing radial basis neuro-fuzzy linear quadratic regulator control of double link rotary pendulum," *Proceedings of the Institution of Mechanical Engineers, Part I: Journal of Systems and Control Engineering*, vol. 236, 09 2021.

[16] Z. B. Hazem, M. J. Fotuhi, and Z. Bingl, "Development of a fuzzy-lqr and fuzzy-lqg stability control for a double link rotary inverted pendulum," *Journal of the Franklin Institute*, vol. 357, no. 15, pp. 10 529–10 556, 2020.

[17] I. Jmel, H. Dimassi, S. Hadj-Said, and F. MSahli, "An adaptive sliding mode observer for inverted pendulum under mass variation and disturbances with experimental validation," *ISA Transactions*, vol. 102, pp. 264–279, 2020.

[18] J. Feng, S. Gao, D. Zhao, X. Yan, and S. K. Spurgeon, "Dynamic output feedback sliding mode control for non-minimum phase systems with application to an inverted pendulum." *IFAC-PapersOnLine*, vol. 53, no. 2, pp. 5165–5170, 2020, 21st IFAC World Congress.

[19] R. Olfati-Saber, "Normal forms for underactuated mechanical systems with symmetry," *IEEE Transactions on Automatic Control*, vol. 47, no. 2, pp. 305–308, Feb. 2002.

[20] M. Anderle, S. Čelikovský, D. Henrion, and J. Zikmund, "LMI based design for the acrobot walking," in *Preprints of the 9th IFAC Symposium on Robot Control*, Gifu, Japan, 2009, pp. 595–600.

[21] M. Anderle and S. Čelikovský, "Analytical design of the Acrobot exponential tracking with application to its walking," in *Proccedings of the IEEE International Conference on Control and Automation, ICCA 2009*, 2009, pp. 163–168.

[22] I. Fantoni and R. Lozano, *Non-linear control of underactuated mechanical systems*. Heidelberg: Springer Verlag, 2002.

[23] W. Greiner, *Classical Mechanics: System of Particles and Hamiltonian Dynamics*. Berlin: Springer Verlag, 2003.

[24] R. Khusainov, S. Mamedov, S. Sellami, and A. Klimchik, "Mechanical design optimization for a five-link walking bipedal robot," *IFAC-PapersOnLine*, vol. 53, no. 2, pp. 8953–8958, 2020, 21st IFAC World Congress.

[25] S. Čelikovský and M. Anderle, "Chain of four integrators as a possible essence of the under-actuated planar walking." *IFAC-PapersOnLine*, vol. 54, no. 14, pp. 60–65, 2021, 3rd IFAC Conference on Modelling, Identification and Control of Nonlinear Systems MICNON 2021.